Chapter 3
Exact Solutions of the Navier–Stokes Equations

In this chapter, we solve a few simple problems of fluid mechanics in order to illustrate the fundamental concepts related to the flow of viscous incompressible fluids. All solutions presented in this chapter are exact solutions of the full Navier Stokes equations. The review article by Ratip Berker [14] constitutes an inexhaustible source of these solutions that cover a wide spectrum of incompressible flows. Another compilation of exact solutions is provided in the book by Drazin and Riley [28].

We first consider steady state plane flows: Couette, Poiseuille and the free surface flow over an inclined plane. Further we treat steady state flows in cylindrical geometry: Couette, Poiseuille and their combination in the helical flow between two circular cylinders in relative rotation. Finally we solve unsteady plane and axisymmetric problems, plane periodic flows and various pipe flows.

3.1 Plane Stationary Flows

Here, we examine some exact solutions of the Navier–Stokes equations for plane stationary flows.

3.1.1 Plane Couette Flow

We consider the two-dimensional stationary flow of an incompressible viscous fluid between parallel plates.

Figure 3.1 shows the flow domain. The lower boundary is fixed while the upper boundary moves in its own plane at a given constant velocity U in the x_1 direction.
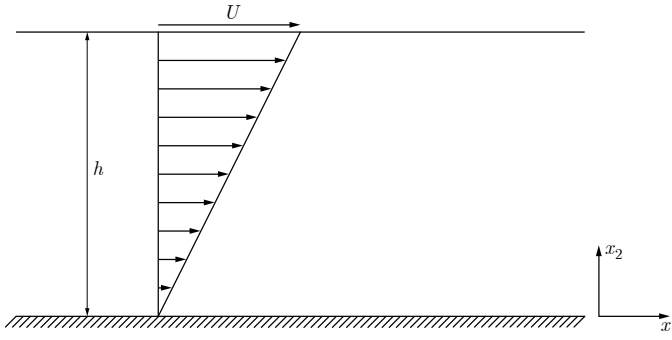
Fig. 3.1 Plane Couette flow

Since the flow is two-dimensional, the vector $\boldsymbol{v}$ reduces to two components, $\boldsymbol{v} = (v_1, v_2, 0)$. We assume that the flow is developed, that is, the transient effects and those from the upstream edges of the plates are negligible. This is a very strong assumption and the subsequent solution is only due to this simplification. In reality a uniform flow impinging on the plates will generate boundary layers where the viscous effects are dominant and after some distance, the layers will merge into the fully viscous solution.

With the previous hypotheses, we can have v_1 as a function only of x_2. The incompressibility condition (1.73) becomes

$$\frac{\partial v_2}{\partial x_2} = 0 \tag{3.1}$$

indicating that v_2 is not a function of x_2; it is thus a function of x_1. However, since at the two boundaries v_2 is zero for all x_1, we conclude that $v_2 = 0$ everywhere. We write the two-dimensional Navier–Stokes equation (1.74) for the velocity component v_1 as

$$\rho\left(\frac{\partial v_1}{\partial t} + v_1\frac{\partial v_1}{\partial x_1} + v_2\frac{\partial v_1}{\partial x_2}\right) = -\frac{\partial p}{\partial x_1} + \mu\triangle v_1 + \rho b_1. \tag{3.2}$$

As the gravitational force is oriented along the negative direction of the axis x_2, $b_1 = 0$. In addition, the problem is stationary, thus $\partial v_1/\partial t = 0$. The term $v_1\partial v_1/\partial x_1$ is zero as $v_1 = v_1(x_2)$. Finally $v_2\partial v_1/\partial x_2$ is also zero since $v_2 = 0$. We can assume that the horizontal component of the pressure gradient is zero as the flow is forced kinematically by the motion of the upper plate. We are left with

$$\mu\frac{d^2 v_1}{dx_2^2} = 0. \tag{3.3}$$

Integrating (3.3) once, we obtain

$$\mu \frac{dv_1}{dx_2} = C \ . \tag{3.4}$$

This relation shows that the shear stress is constant across the height of the channel. Integrating again leads to

$$v_1 = Ax_2 + B. \tag{3.5}$$

The adherence boundary conditions

$$v_1(x_2 = 0) = 0, \ v_1(x_2 = h) = U \tag{3.6}$$

permit us to determine the integration constants; we obtain a linear velocity profile

$$v_1 = \frac{Ux_2}{h}. \tag{3.7}$$

The shear stress component (1.67) obtained with (3.7) is a constant

$$\sigma_{12} = \mu \frac{dv_1}{dx_2} = \mu \frac{U}{h} \ . \tag{3.8}$$

If we examine the second Navier–Stokes equation, in direction x_2, we have

$$0 = -\frac{\partial p}{\partial x_2} - \rho g, \tag{3.9}$$

with g the gravitational acceleration. Integrating this relation and taking into account the independence of p with respect to x_1, leads to

$$p = -\rho g x_2 + C. \tag{3.10}$$

As the pressure in an incompressible fluid is only known to an arbitrary constant, we choose it by imposing $p(x_2 = h) = 0$ which yields $C = \rho g h$. The pressure is in hydrostatic equilibrium

$$p = \rho g(h - x_2) \ . \tag{3.11}$$

3.1.2 *Plane Poiseuille Flow*

Consider the two-dimensional stationary flow of a viscous incompressible fluid in a channel formed by two fixed walls. Figure 3.2 shows the geometric configuration of the domain. In this case, a longitudinal pressure gradient, along direction x_1, is established. We assume that the flow is developed and that the fluid particles move on paths parallel to the walls. Reasoning as for Couette flow, we can write $v_1 = v_1(x_2), \ v_2 = 0$.
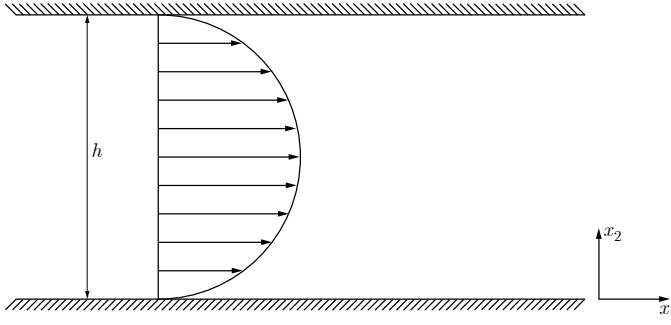
Fig. 3.2 Plane Poiseuille flow

The dynamic equation for velocity v_1 is relation (1.74), which for Poiseuille flow reduces to

$$0 = -\frac{\partial p}{\partial x_1} + \mu \frac{\partial^2 v_1}{\partial x_2^2} \ . \tag{3.12}$$

As for Couette flow, the pressure in the vertical direction is in hydrostatic equilibrium

$$0 = -\frac{\partial p}{\partial x_2} - \rho g \ . \tag{3.13}$$

Integrating this relation, we obtain

$$p = -\rho g x_2 + P(x_1) \ . \tag{3.14}$$

The integration factor, $P(x_1)$, is the pressure on the lower wall, for $x_2 = 0$. The pressure gradient in direction x_1 can be written as

$$\frac{\partial p}{\partial x_1} = \frac{dP}{dx_1} \ , \tag{3.15}$$

as it is a function only of x_1. Equation (3.12) yields

$$\frac{d^2 v_1}{dx_2^2} = \frac{1}{\mu} \frac{dP}{dx_1} = C. \tag{3.16}$$

We note that the first term is a function of x_2 while the second is a function of x_1. It follows that these two terms must be equal to the same constant C. The integration of (3.16) gives us

$$v_1 = \frac{1}{\mu} \frac{dP}{dx_1} \frac{x_2^2}{2} + A x_2 + B. \tag{3.17}$$

Imposing the boundary conditions

$$v_1(x_2 = 0) = v_1(x_2 = h) = 0, \tag{3.18}$$

yields the parabolic Poiseuille velocity profile

$$v_1 = -\frac{h^2}{2\mu} \frac{dP}{dx_1} \frac{x_2}{h} (1 - \frac{x_2}{h}). \tag{3.19}$$

As the pressure in the channel diminishes linearly with distance x_1, $dP/dx_1 < 0$, and the flow is in the positive x_1 direction.

The shear stress component obtained from (3.19) is

$$\sigma_{12} = \mu \frac{dv_1}{dx_2} = -\frac{h}{2} \frac{dP}{dx_1} (1 - \frac{2x_2}{h}). \tag{3.20}$$

We note that the shear (3.20) is zero on the symmetry axis of the channel, $x_2 = h/2$, and the absolute value is at a maximum on both walls.

We can calculate the volume flux or flow rate through the section S of the channel. The general definition of the volume flux is given by the relation

$$Q = \int_S \boldsymbol{v} \cdot \boldsymbol{n} \, dS . \tag{3.21}$$

Considering a unit surface in direction x_3, the flow rate in the two-dimensional channel is written

$$Q = \int_0^h v_1 \, dx_2 = -\frac{h^3}{12\mu} \frac{dP}{dx_1} = \frac{h^3}{12\mu} \frac{\triangle p}{L}, \tag{3.22}$$

with $\triangle P$ the pressure difference observed at two points with the same ordinate, x_2, separated by a distance L in direction x_1. We define the average velocity by $Q = v_{avg} h$, from which we have

$$v_{avg} = \frac{h^2}{12\mu} \frac{\triangle P}{L}. \tag{3.23}$$

As the maximum velocity, v_{max}, is attained on the axis of symmetry of the channel, at $x_2/h = 1/2$, it follows that

$$v_{max} = \frac{h^2}{8\mu} \frac{\triangle P}{L} \tag{3.24}$$

and, consequently

$$v_{avg} = \frac{2}{3} v_{max}. \tag{3.25}$$

In the case where the two-dimensional channel is replaced by a pipe with circular section (see Sect. 3.2.2), we obtain the average velocity equal to half the maximum velocity. This shows that the zone of high velocity constitutes a smaller fraction of the section.

Another way of solving the plane Poiseuille flow consists in moving the origin of the coordinate axes to mid-channel height and locate the two channel planes at $x_2 = \pm h$. The governing equation is still (3.12) with the solution given by (3.17). Now the boundary conditions are

$$v_1(x_2 = \pm h) = 0 . \tag{3.26}$$

It is left as an exercise to the reader to perform the algebra. Setting $-dP/dx_1 = G$, one gets the parabolic profile

$$v_1 = \frac{G}{2\mu}\left(h^2 - x_2^2\right) = \frac{Gh^2}{2\mu}\left(1 - \frac{x_2^2}{h^2}\right) , \tag{3.27}$$

which will be useful in the pipe flow section.

3.1.3   Flow of an Incompressible Fluid on an Inclined Plane

We have a stationary, two-dimensional flow of a viscous Newtonian fluid on a plane inclined at angle α to the vertical (Fig. 3.3). The thickness of the fluid layer is uniform and equal to h. At the free surface, the fluid is in contact with ambient air which we consider to be a perfect fluid at atmospheric pressure p_a. We assume that the flow in the air does not affect the flow of the viscous fluid. The flow is parallel because the trajectories of the fluid particles are parallel to the inclined plane. Then, $\mathbf{v} = (v_1, 0, 0)$. From incompressibility we obtain

$$\frac{\partial v_1}{\partial x_1} = 0, \tag{3.28}$$

therefore we deduce that $v_1 = v_1(x_2)$. The only components of the stress tensor are σ_{12} or σ_{21}. As the pressure is uniform at the free surface, the pressure in the viscous fluid can not depend on direction x_1, but only on x_2.
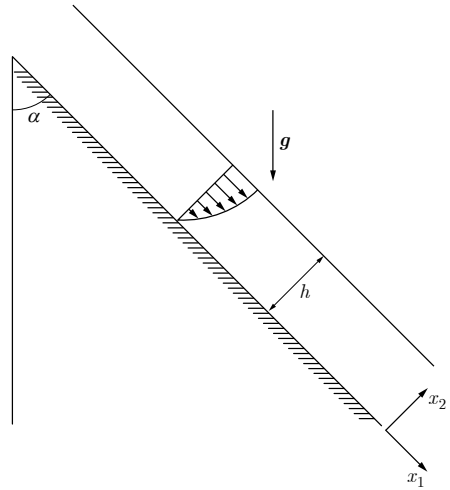
From the motion equation (1.58), written in direction x_1, it follows that

$$\frac{\partial \sigma_{12}}{\partial x_2} + \rho b_1 = \frac{\partial \sigma_{12}}{\partial x_2} + \rho g \cos\alpha = 0 . \tag{3.29}$$

Integrating this relation, we have

$$\sigma_{12} = -\rho g \, x_2 \cos\alpha + C . \tag{3.30}$$

Fig. 3.3 Flow on an inclined
plane

At the free surface, $x_2 = h$, the shear stress should be zero. We obtain

$$\sigma_{12} = \rho g \cos \alpha (h - x_2) \, . \tag{3.31}$$

As $\sigma_{12} = \mu \, dv_1/dx_2$, we can evaluate the component v_1 by integrating with respect to x_2, taking into account the boundary condition $v_1(x_2 = 0) = 0$. The velocity profile is given by the relation

$$v_1 = \frac{\rho g \cos \alpha}{2\mu} x_2 (2h - x_2) \, . \tag{3.32}$$

The Navier–Stokes equation for direction x_2 yields the relation

$$-\frac{\partial p}{\partial x_2} + \rho b_2 = -\frac{\partial p}{\partial x_2} - \rho g \sin \alpha = 0 \, . \tag{3.33}$$

Integrating with respect to x_2 and taking into account the condition on the free surface $p(x_2 = h) = p_a$, we can write

$$p = p_a - (\rho \, g \sin \alpha)(x_2 - h) \, . \tag{3.34}$$

The flow rate per unit length in direction x_3 is obtained from

$$Q = \int_0^h v_1 \, dx_2 = \frac{\rho g \cos \alpha \, h^3}{2\mu} \, . \tag{3.35}$$

3.2   Axisymmetric Stationary Flows

In this section, we consider exact solutions of the Navier–Stokes equations for stationary flows in axisymmetric geometries of revolution. We integrate the Navier–Stokes equations expressed in a cylindrical coordinate system. The vector velocity has components v_r, v_θ, and v_z which we call the radial, azimuthal, and axial velocities, respectively.

3.2.1   Circular Couette Flow

Consider the stationary flow of an incompressible viscous Newtonian fluid between two concentric cylinders supposed to be of infinite axial length. We denote by R_1 and R_2 the radii of the internal and external cylinders, respectively, and ω_1 and ω_2 their respective rates of angular rotation, as shown in Fig. 3.4. We want to calculate the azimuthal velocity v_θ. This flow is known by the name of circular Couette flow. We neglect the effects of the volume forces. The flow has no axial velocity since there is no pressure gradient in that direction. In addition, due to the symmetry of revolution, it also does not depend on the azimuthal coordinate, thus $\partial(\bullet)/\partial\theta = 0$. The two velocity components v_r and v_θ, stationary, thus independent of time, are functions uniquely of the radial coordinate, r, so $v_r = v_r(r)$ and $v_\theta = v_\theta(r)$. Applying adherence to the wall, the boundary conditions are

$$v_r(R_1) = v_r(R_2) = 0, \quad v_\theta(R_1) = \omega_1 R_1, \ v_\theta(R_2) = \omega_2 R_2 . \qquad (3.36)$$

With these assumptions about the velocity profile, the continuity Eq. (A.20) becomes

$$\frac{1}{r}\frac{d}{dr}(r\,v_r) = 0 . \qquad (3.37)$$

Taking into account the condition (3.36) that v_r is zero at the boundaries, the solution is
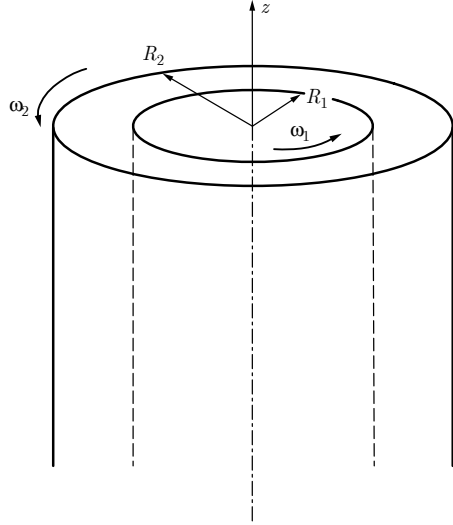
$$v_r = 0 . \qquad (3.38)$$

In this case the Navier–Stokes equations (A.21)–(A.22) reduce to

$$\frac{\partial p}{\partial r} = \rho\,\frac{v_\theta^2}{r} , \qquad (3.39)$$

$$\frac{1}{r}\frac{\partial}{\partial r}\left(r\,\frac{\partial v_\theta}{\partial r}\right) - \frac{v_\theta}{r^2} = 0 . \qquad (3.40)$$

Fig. 3.4 Circular Couette flow

The solution for the component v_θ is in the form

$$v_\theta = \sum_{n=-\infty}^{n=+\infty} a_n r^n \; .$$

Plugging this series into (3.40), we easily find that $n = \pm 1$. Imposing the boundary conditions leads to

$$v_\theta = Ar + \frac{B}{r} = \frac{\omega_2 R_2^2 - \omega_1 R_1^2}{R_2^2 - R_1^2} \, r - \frac{(\omega_2 - \omega_1) R_1^2 R_2^2}{R_2^2 - R_1^2} \, \frac{1}{r} \tag{3.41}$$

after solving for the constants A and B. The first term on the right-hand side corresponds to rotation of all the fluid around the central axis. If $\omega_1 = \omega_2 = \omega$, the velocity becomes $v_\theta = \omega r$, which shows that the fluid rotates as a rigid body around the axis. The second term on the right-hand side corresponds to a deformation of the particles over time. If $R_2 \to \infty$ and $\omega_2 = 0$, then we have the case of a cylinder in an infinite fluid. The velocity $v_\theta = \omega_1 R_1^2 / r$ gives circular streamlines around the cylinder, and the velocity distribution is irrotational, that is, **curl v = 0**.

The pressure in the Couette flow is computed from Eq. (3.39). After integration, we obtain

$$\frac{p(r)}{\rho} = \frac{p(R_1)}{\rho} + \frac{(R_2^2 \omega_2 - R_1^2 \omega_1)^2}{(R_2^2 - R_1^2)^2} \frac{r^2 - R_1^2}{2} - \frac{R_1^4 R_2^4 (\omega_2 - \omega_1)^2}{2(R_2^2 - R_1^2)^2} \left(\frac{1}{r^2} - \frac{1}{R_1^2} \right)$$
$$+ \frac{2(R_2^2 \omega_2 - R_1^2 \omega_1) R_1^2 R_2^2 (\omega_1 - \omega_2)}{(R_2^2 - R_1^2)^2} \ln \left(\frac{r}{R_1} \right) \; . \tag{3.42}$$

A tangential shear stress $\sigma_{\theta r}$ acts on a surface element with a radial normal, which is expressed by (A.5)

$$\sigma_{\theta r} = \mu \left(\frac{\partial v_\theta}{\partial r} - \frac{v_\theta}{r} + \frac{1}{r} \frac{\partial v_r}{\partial \theta} \right) = \mu \left(\frac{\partial v_\theta}{\partial r} - \frac{v_\theta}{r} \right) = \mu\, r\, \frac{\partial}{\partial r} \left(\frac{v_\theta}{r} \right) . \qquad (3.43)$$

Combining (3.41) and (3.43), we obtain

$$\sigma_{\theta r} = -\frac{2B\mu}{r^2} . \qquad (3.44)$$

Next we calculate the viscous moment, M, that acts on the interior cylinder per unit axial length. This moment is equal to the component $\sigma_{\theta r}$ evaluated at $r = R_1$ and the area, $2\pi R_1$, on which this stress acts, multiplied by the lever arm, R_1, the distance between the axis and the point where the force acts. We have

$$M = -2\pi R_1^2 \frac{2B\mu}{R_1^2} = 4\pi\mu \frac{(\omega_2 - \omega_1) R_1^2 R_2^2}{R_2^2 - R_1^2} . \qquad (3.45)$$

This last relation indicates that we can measure the viscosity μ of a fluid in a Couette viscometer where the drive motor imposes a torque on one of the cylinders and we measure the resulting rotation speed of the other one.

3.2.2 Circular Poiseuille Flow in a Cylindrical Pipe

Poiseuille flow in a circular pipe with radius R is subject to the action of an imposed pressure gradient in direction z (Fig. 3.5). The flow is stationary. From the Navier–Stokes equations in cylindrical coordinates, we show first that the only non-zero component of the velocity is v_z.
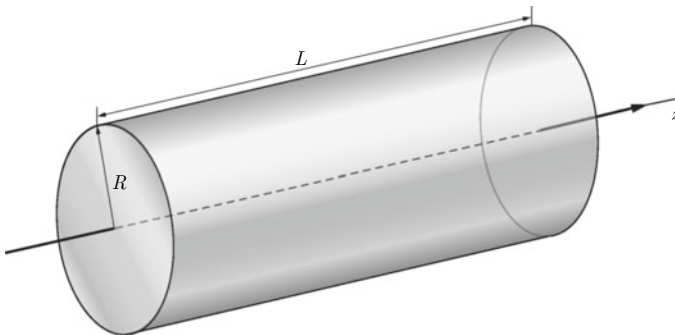

Fig. 3.5 Circular Poiseuille flow in a cylindrical pipe

Given the hypotheses of axial symmetry and stationary flow, $v_\theta = 0$ and the only two components of velocity, v_r and v_z, are functions only of r. The continuity Eq. (A.20) is then

$$\frac{1}{r}\frac{\partial}{\partial r}(r\, v_r) = 0 \,. \tag{3.46}$$

Integration yields

$$r v_r = f(z) \,.$$

But, since $v_r = 0$ at the wall, $r = R$, we conclude that $f(z) = 0$ and thus that v_r is zero everywhere in the flow. The Navier–Stokes equation for the radial component of velocity (A.21) reduces to $\partial p/\partial r = 0$. The pressure depends only on z and not on r. The equation for the velocity component v_z (A.23) yields

$$-\frac{dp}{dz} + \mu\left(\frac{\partial^2 v_z}{\partial r^2} + \frac{1}{r}\frac{\partial v_z}{\partial r}\right) = 0$$

or

$$\frac{dp}{dz} = \frac{\mu}{r}\frac{d}{dr}\left(r\,\frac{dv_z}{dr}\right) \,.$$

The left-hand side term only depends on z; on the right-hand side there is only dependence on r. Thus the two terms must be equal to a constant. Integrating, we obtain

$$v_z = \left(\frac{dp}{dz}\right)\frac{1}{\mu}\left(\frac{r^2}{4} + A\ln r + B\right) \,.$$

The velocity must be finite on the axis $r = 0$. This leads to $A \equiv 0$. Taking into account the condition $v_z(R) = 0$, we have

$$v_z = -\left(\frac{dp}{dz}\right)\frac{R^2}{4\mu}\left(1 - \left(\frac{r}{R}\right)^2\right) = \frac{GR^2}{4\mu}\left(1 - \frac{r^2}{R^2}\right) \,, \tag{3.47}$$

with the definition $dp/dz = -G$. In Poiseuille flow, the velocity profile is parabolic. The maximum velocity at the center is

$$v_{max} = -\left(\frac{dp}{dz}\right)\frac{R^2}{4\mu} \,. \tag{3.48}$$

Therefore the parabolic profile may be written

$$v_z = v_{max} \left(1 - \frac{r^2}{R^2} \right) . \tag{3.49}$$

The flow rate is obtained by integration over the section of the pipe. We have

$$Q = 2\pi \int_0^R v_z(r)\, r\, dr = -\left(\frac{dp}{dz} \right) \frac{\pi R^4}{8\mu} = \frac{\pi R^2 v_{max}}{2} . \tag{3.50}$$

The average, or flux, velocity obtained from the flux divided by the area of the section S is

$$v_{avg} = \frac{Q}{S} = \frac{v_{max}}{2} . \tag{3.51}$$

The maximum velocity is thus equal to twice the average velocity. The shear stress at the cylinder wall, which we denote τ_w, is given by the component σ_{zr} evaluated at $r = R$

$$\tau_w = -\mu \frac{dv_z}{dr} \mid_{r=R} = -\left(\frac{dp}{dz} \right) \frac{R}{2} = \frac{2\mu v_{max}}{R} = \frac{4\mu v_{avg}}{R} . \tag{3.52}$$

The sign change between τ_w and σ_{zr} comes from the fact that τ_w represents the shear force exercised on the wall by the fluid. The friction coefficient is defined by the ratio of the stress at the wall to the average dynamic pressure

$$C_f = \frac{\tau_w}{\frac{\rho v_{avg}^2}{2}} = \frac{8\mu}{\rho R v_{avg}} = \frac{8\nu}{R v_{avg}} = \frac{16}{Re_D} , \tag{3.53}$$

with Re_D being the Reynolds number based on the average velocity and the diameter of the section. It is common to define the head loss coefficient λ by the relation

$$-\left(\frac{dp}{dz} \right) = \frac{\rho v_{avg}^2}{2} \frac{\lambda}{D} . \tag{3.54}$$

Thus it follows that

$$\lambda = 4C_f = \frac{64}{Re_D} . \tag{3.55}$$

3.2.3 Helical Flow Between Two Circular Cylinders in Relative Motion

From the geometry point of view, this flow occurs in a configuration similar to the circular Couette flow in Fig. 3.4, with the same notation R_1 and R_2 for the radii and ω_1, ω_2 for the angular rates of rotation. Furthermore the viscous fluid between the cylinders is subjected to an axial pressure gradient. As the flow is steady-state,

$\partial/\partial t = 0$, and axisymmetric, $\partial/\partial\theta = 0$, the velocity profile is a function of r only. One has

$$v_r = v_r(r), \ v_\theta = v_\theta(r), \ v_z = v_z(r), \ p = p(r, z) \ . \tag{3.56}$$

With the fluid adherence to the wall, the boundary conditions are

$$v_r(R_1) = v_r(R_2) = 0, \quad v_\theta(R_1) = \omega_1 R_1, \ v_\theta(R_2) = \omega_2 R_2,$$
$$v_z(R_1) = v_z(R_2) = 0 \ . \tag{3.57}$$

Similarly to the Couette flow solution, it is easy to show that the v_r component is zero everywhere. The Navier–Stokes equations (A.21)–(A.23) become

$$\frac{1}{\rho}\frac{\partial p}{\partial r} = \frac{v_\theta^2}{r} \ , \tag{3.58}$$

$$\frac{1}{r}\frac{\partial}{\partial r}\left(r\frac{\partial v_\theta}{\partial r}\right) - \frac{v_\theta^2}{r} = 0 \ , \tag{3.59}$$

$$-\frac{\partial p}{\partial z} + \mu\left(\frac{\partial^2 v_z}{\partial r^2} + \frac{1}{r}\frac{\partial v_z}{\partial r}\right) = 0. \tag{3.60}$$

The Couette solution (3.41) remains valid. Equation (3.58) yields

$$p = \rho\int_{R_1}^r \frac{v_\theta^2}{r'}dr' + f(z) \ , \tag{3.61}$$

where v_θ is the Couette profile and $f(z)$ is an indeterminate function of z. Introducing (3.61) in (3.60), one gets

$$-\frac{df}{dz} + \mu\frac{1}{r}\frac{d}{dr}\left(r\frac{dv_z}{dr}\right) = 0 \ . \tag{3.62}$$

The solutions are obtained taking the boundary conditions (3.57) into account

$$f(z) = -Az + B \ , \tag{3.63}$$

$$v_z(r) = \frac{A}{4\mu}\left[-r^2 + \frac{R_2^2 - R_1^2}{\ln(R_2/R_1)}\ln r + \frac{R_1^2\ln R_2 - R_2^2\ln R_1}{\ln(R_2/R_1)}\right] \ . \tag{3.64}$$

The pressure field is given by

$$p(r, z) = \rho\int_{R_1}^r \frac{v_\theta^2}{r'}dr' - Az + B. \tag{3.65}$$

The pressure is known up to a constant B, which will give the reference pressure; the pressure gradient $-A$ acts in the direction of the axis and finally, the first term

of the right hand side member of (3.65) equilibrates the centrifugal forces of the rotating fluid. Note that the axial velocity is independent of the rotation speed of the cylinders, while the azimuthal velocity v_θ is independent of the pressure gradient.

3.3 Plane Transient Flows

Let us now turn our attention to plane flows that depend on time. This situation leads to partial differential equations with independent variables of space and time. In order to arrive at an analytic solution of the problem, we use a change of variables to obtain an ordinary differential equation that is easier to solve.

3.3.1 Transient Flow in a Semi-infinite Space

An incompressible Newtonian viscous fluid occupies a half space ($x_2 \geq 0$), and is at rest for $t < 0$ (Fig. 3.6). At time $t = 0$, the rigid plane which limits the half space is instantaneously set into motion at the constant velocity U in the positive direction of axis x_1. The motion is two-dimensional such that $v_3 = 0$.

The boundary and initial conditions are given by

$$t < 0, \quad v_1 = v_2 = 0, \quad \forall x_1, x_2 \tag{3.66}$$

$$t \geq 0, \quad v_1 = U, v_2 = 0, \text{ for } x_2 = 0, \tag{3.67}$$

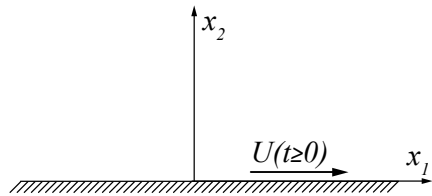$$v_1 = v_2 = 0, \text{ for } x_2 \to \infty. \tag{3.68}$$

We assume that v_1 and v_2 are functions of x_2 and t

$$v_1 = v_1(x_2, t), \ v_2 = v_2(x_2, t) , \tag{3.69}$$

and that the pressure p is a function only of x_2 (there is no horizontal pressure gradient; the flow is generated entirely by the motion of the moving wall). The conservation of mass becomes

$$\frac{\partial v_2(x_2, t)}{\partial x_2} = 0 . \tag{3.70}$$

Fig. 3.6 Unsteady flow in an infinite half space

The component v_2 only depends on time, and with conditions (3.67) and (3.68), it is identically zero for all t. The Navier–Stokes equations become

$$\rho \frac{\partial v_1}{\partial t} = \mu \frac{\partial^2 v_1}{\partial x_2^2} \,, \tag{3.71}$$

$$\frac{\partial p}{\partial x_2} = 0 \,. \tag{3.72}$$

The pressure p is constant.

We can, if we wish, include the effect of gravity in the pressure calculation, by writing

$$\frac{\partial p}{\partial x_2} = -\rho g x_2 \,. \tag{3.73}$$

Integration of this relation leads to the calculation of the hydrostatic pressure, where the pressure at a point is equal to the weight of the column of fluid located above that position. The hydrostatic pressure, as its name suggests, does not participate in the dynamics of the flow.

The motion equation (3.71) is a diffusion equation, of the same type as the "heat equation". We can transform this partial differential equation into an ordinary differential equation with a variable change that we obtain from dimensional analysis (cf. Sect. 2.5). Since the problem has no spatial scale other than the variable x_2 nor time scale other than that of t itself, we combine them to form the non-dimensional group (compare with Eq. (2.36))

$$\eta = \frac{x_2}{2\sqrt{\nu t}} \,. \tag{3.74}$$

This permits us to obtain an ordinary differential equation for which the solution is a function of η. It is called a self-similar solution because the velocity profile with respect to the variable x_2 is similar for all times t.

Setting

$$v_1 = U \, f(\eta) \,, \tag{3.75}$$

relation (3.71) becomes

$$f'' + 2\eta f' = 0 \,, \tag{3.76}$$

with conditions

$$\eta = 0, \, f = 1; \quad \eta \to \infty, \, f = 0 \,. \tag{3.77}$$

Integrating (3.76), we obtain

$$f = A \int_0^\eta e^{-\eta'^2} d\eta' + B \,. \tag{3.78}$$

Taking into account conditions (3.77), we have for $\eta = 0$, $B = 1$ and for $\eta = \infty$, $A = -2/\sqrt{\pi}$ where we introduced the error function erf(x) defined by Abramowitz and Stegun [1]

$$\text{erf}(x) = \frac{2}{\sqrt{\pi}} \int_0^x e^{-\tau^2} d\tau , \qquad (3.79)$$

such that $\text{erf}(\infty) = 1$. Then

$$f = 1 - \text{erf}\,\eta , \qquad (3.80)$$

and from (3.75) the velocity of the fluid for $t > 0$ is

$$v_1 = U[1 - \text{erf}(\frac{x_2}{2\sqrt{vt}})] . \qquad (3.81)$$

The velocity profile v_1/U as a function of η is shown in Fig. 3.7. For a fixed value of t, the variable η is proportional to x_2. Then, we can deduce the velocity profile at every instant as a function of the distance from the wall. An interesting question is to know the depth of penetration of the wall motion into the semi-infinite space. More precisely, for a given t, what is the distance at which the velocity attains, for example, one per cent of the value of U? Examining the function erf, $1 - \text{erf}$ has the value 0.01 for $\eta \sim 2$. Defined as such, the penetration depth δ is given by

$$\eta_\delta = \frac{\delta}{2\sqrt{vt}} \simeq 2, \quad \delta \simeq 4\sqrt{vt} , \qquad (3.82)$$

which is proportional to the square root of the kinematic viscosity and time. If the viscosity is very small, the fluid "sticks" less to the wall and it has a weak effect. If t tends to infinity, the velocity at every point in the half space goes to U.

3.3.2 Flow on an Oscillating Plane

Consider the flow produced by the periodic horizontal oscillation of a plate in its own plane (Fig. 3.8).

Equation (3.71) still applies, and we must solve it with the boundary conditions

$$v_1 = U \cos \omega t \quad \text{for} \quad x_2 = 0 . \qquad (3.83)$$

After the initial transient phenomena, the fluid velocity gradually becomes a periodic function of time at the same frequency as the plate oscillation. Here we examine this periodic regime. Assume that solution v_1 is of the form

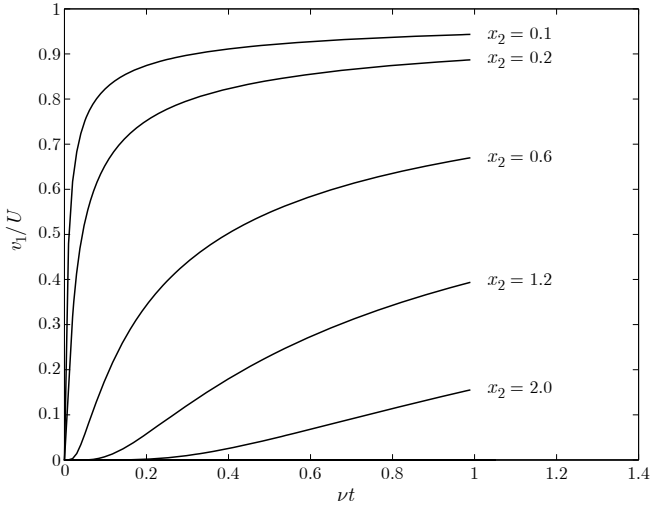$$v_1 = \Re \left(e^{i\omega t} f(x_2) \right) , \qquad (3.84)$$

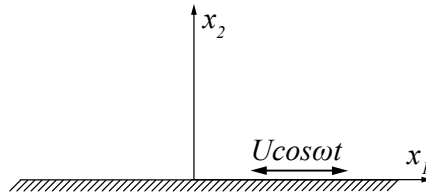**Fig. 3.7** Transient flow in an infinite half space

Fig. 3.8 Unsteady flow on an oscillating plane

where $\Re$ means the real part of a complex expression. The combination of (3.71) and (3.84) yields

$$i\omega f = v\frac{d^2 f}{dx_2^2} \; .$$

Recall that $i^{1/2} = e^{i\pi/4}$; then the only solution that remains finite as $x_2 \to \infty$ is

$$f = A \exp\left(-(1+i)(\omega/2v)^{1/2}x_2\right) \; .$$

The imposition of the boundary condition (3.83) leads to $A = U$ and the solution becomes

$$v_1 = U \exp\left(-(\omega/2v)^{1/2}x_2\right)\cos\left(\omega t - (\omega/2v)^{1/2}x_2\right) \; . \tag{3.85}$$

The velocity profile is a damped harmonic oscillation of amplitude $Ue^{-x_2\sqrt{\omega/2v}}$ in a fluid where a layer at distance x_2 has a phase lag of $x_2\sqrt{\omega/2v}$ with respect to the motion at the wall. Two layers of fluid separated by the distance $2\pi(2v/\omega)^{1/2}$

oscillate in phase. This distance constitutes an estimation of the length of the motion and is called the viscous wave penetration depth. That it increases with viscosity and decreases with frequency is not surprising: if we slowly oscillate a flat plate in a sticky fluid, we expect to drag large masses of fluid along with the plate; on the other hand, if we move the plate rapidly in a fluid of low viscosity, we expect the fluid essentially to ignore the plate, except in a thin boundary layer.

3.3.3   Channel Flow with a Pulsatile Pressure Gradient

Blood flow in the vascular tree is driven by the pulsating pressure gradient produced by the heart that is acting as a pump. In order to avoid (temporarily) the geometrical complexity of cylindrical coordinates of blood flow in the arteries, we will tackle a simplified version of the problem, namely the plane channel flow under an oscillating pressure gradient.

Recall that the standard plane Poiseuille flow as shown in Fig. 3.2 with a steady constant pressure gradient denoted by G gives rise to a parabolic velocity profile. Let us add now an oscillating component characterized by the pulsation ω such that

$$-\frac{1}{\rho}\frac{\partial p}{\partial x_1} = -G - C\cos\omega t \ , \tag{3.86}$$

with C a constant obtained from experimental data, for example. For the sake of simplicity in the analytical treatment, it is customary to resort to Fourier representation and use the relation

$$-\frac{1}{\rho}\frac{\partial p}{\partial x_1} = -G - \Re(Ce^{i\omega t}) \ . \tag{3.87}$$

As the steady state oscillating solution is sought for the velocity field, the solution is written as a complex function

$$v_1 = v_P + \Re\left(u(\omega, x_2)e^{i\omega t}\right) \ . \tag{3.88}$$

where the Poiseuille solution v_P given by Eq. (3.27) corresponds to the constant pressure gradient.

The Navier–Stokes equations lead to the relation

$$\frac{\partial v_1}{\partial t} = -\frac{1}{\rho}\frac{\partial p}{\partial x_1} + \nu\frac{\partial^2 v_1}{\partial x_2^2} \ . \tag{3.89}$$

With Eqs. (3.87) and (3.88), Eq. (3.89) gives

$$i\omega u = -C + \nu\frac{\partial^2 u}{\partial x_2^2} \ . \tag{3.90}$$

The boundary conditions are

$$u(h) = 0, \quad \frac{\partial u}{\partial x_2}(0) = 0 . \tag{3.91}$$

The solution of (3.90) is

$$u = \Re \left[\frac{iC}{\omega} \left(1 - \frac{\cosh \sqrt{\frac{i\omega}{\nu}} x_2}{\cosh \sqrt{\frac{i\omega}{\nu}} h} \right) \right] . \tag{3.92}$$

Taking the relation $i^{1/2} = (1 + i)/\sqrt{2}$ into account, the real part of (3.92) yields the velocity field

$$v_1 = v_P - \frac{C}{\omega} \left[\left(1 - \frac{f_1(\omega, x_2)}{f_3(kh)} \right) \sin \omega t - \frac{f_2(\omega, x_2)}{f_3(kh)} \cos \omega t \right] , \tag{3.93}$$

where the various notations are defined as follows

$$\begin{aligned}
k &= \sqrt{\frac{\omega}{2\nu}} , \\
cc(x) &= \cos(x) \cosh(x) , \\
ss(x) &= \sin(x) \sinh(x) , \\
f_1(\omega, x_2) &= cc(kx_2)cc(kh) + ss(kx_2)ss(kh) , \\
f_2(\omega, x_2) &= cc(kx_2)ss(kh) - ss(kx_2)cc(kh) , \\
f_3(\omega) &= cc^2(x) + ss^2(x) .
\end{aligned} \tag{3.94}$$

With $\omega = 1$, in Fig. 3.9, the left part represents the flow for a low frequency case or when the viscous forces are important, i.e. $hk \ll 1$, whereas the right part corresponds to high frequency forcing or to a fluid with very low viscosity. The low frequency solution may be obtained by taking the limit of Eq. (3.93) when $k \to 0$. In that limit, $cc(x) \to 1$, $ss(x) \to x^2$ and therefore, one has

$$v_1 = v_P + \frac{Ch^2}{2\nu} \cos \omega t \left(1 - (\frac{x_2}{h})^2 \right) , \tag{3.95}$$

such that the pulsating term is still a parabola with a modified amplitude. The high frequency case or the equivalent inviscid fluid may be treated with the limit $hk \gg 1$. Then $cc(x) \to \frac{1}{2}e^x \cos x$ and $ss(x) \to \frac{1}{2}e^x \sin x$. The limit solution reads

$$v_1 = v_P - \frac{C}{\omega} \left(\sin \omega t - \sin(\omega t - \eta)e^{-\eta} \right) , \tag{3.96}$$
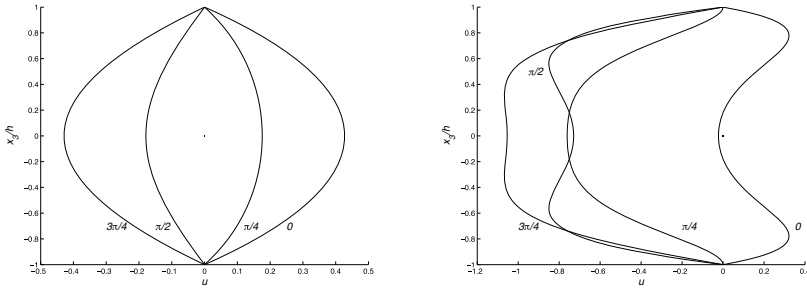
where the new variable η is defined as

Fig. 3.9 Pulsating velocity field with $\omega = 1$; *left*: $k = 1/\sqrt{2}$; *right*: $k = 5/\sqrt{2}$

$$\eta = k(h - x_2) = \frac{h - x_2}{\sqrt{2\nu/\omega}} \ . \tag{3.97}$$

Note that the first term of the oscillating part is the response of the inviscid fluid ($\nu = 0$) to the pressure gradient.

3.4 Axisymmetric Transient Flows

This section treats time dependent flows. The first case is the starting process from rest in a circular Poiseuille flow when the pressure gradient is applied at the initial time. The second example is the pulsating flow in a circular rigid pipe which is somehow connected to blood flow simulation.

3.4.1 Starting Transient Poiseuille Flow

We examine the transient flow in a circular pipe where the fluid starts from rest to reach the Poiseuille steady parabolic profile (3.47). The only non vanishing velocity component is v_z and the pressure gradient goes instantaneously at $t = 0$ from zero to the value $-G$ everywhere. The dynamic equation is from (A.23)

$$G + \mu \left(\frac{\partial^2 v_z}{\partial r^2} + \frac{1}{r} \frac{\partial v_z}{\partial r} \right) = \rho \frac{\partial v_z}{\partial t} \ , \tag{3.98}$$

with the initial condition

$$v_z(r, 0) = 0, \quad 0 \leq r \leq R \ , \tag{3.99}$$

and the boundary condition

$$v_z(R, t) = 0, \forall t . \tag{3.100}$$

In order to render (3.98) homogeneous, let us change variables

$$w(r, t) = \frac{G}{4\mu} \left(R^2 - r^2\right) - v_z(r, t) . \tag{3.101}$$

The new variable will be solution of the equation

$$\frac{\partial^2 w}{\partial r^2} + \frac{1}{r} \frac{\partial w}{\partial r} = \frac{1}{\nu} \frac{\partial w}{\partial t} , \tag{3.102}$$

with the initial condition

$$w(r, 0) = \frac{G}{4\mu} \left(R^2 - r^2\right), \tag{3.103}$$

and the boundary condition

$$w(R, t) = 0, \quad \forall t . \tag{3.104}$$

Through the transient phase, the velocity v_z will increase till the steady state (3.47) is reached, whereas the transient perturbation $w(r, t)$ will decay to zero. To solve (3.102), we proceed by separation of variables

$$w(r, t) = f(r)g(t) . \tag{3.105}$$

Substituting in (3.102), one gets

$$\frac{dg(t)}{dt} + C\nu \, g(t) = 0 , \tag{3.106}$$

$$\frac{d^2 f}{dr^2} + \frac{1}{r} \frac{df}{dr} + C f = 0 , \tag{3.107}$$

where C is an arbitrary constant. The solution of (3.106) reads

$$g(t) = B \exp(-C\nu t) . \tag{3.108}$$

As $w(r, t)$ decreases with respect to time, we assume that C will involve only positive values so that C can be written λ^2/R^2. This notation will ease the next computations, as we will observe. Equation (3.107) then becomes

$$\frac{d^2 f}{dr^2} + \frac{1}{r} \frac{df}{dr} + \frac{\lambda^2}{R^2} f = 0 . \tag{3.109}$$

The change of variable $\lambda r/R = z$ leads (3.109) to the canonical form of the Bessel equation (C.1) whose general solution is given by Eq. (C.2) with the Bessel functions J_k and Y_k. Consequently, the solution of (3.109) is

$$f = C_1 J_0(\frac{\lambda r}{R}) + C_2 Y_0(\frac{\lambda r}{R}) . \tag{3.110}$$

As Y_0 goes to $-\infty$ when $r \to 0$, one concludes that $C_2 \equiv 0$ for w to remain finite on the axis. The general solution of (3.102) becomes

$$w(r, t) = C_3 J_0(\frac{\lambda r}{R}) \exp(-\frac{\lambda^2}{R^2} \nu t) . \tag{3.111}$$

The solution (3.111) verifies condition (3.104) for λ values, denoted λ_n, given by the zeroes of the Bessel function J_0

$$J_0(\lambda_n) = 0 . \tag{3.112}$$

The solution is obtained as

$$w(r, t) = \frac{G}{4\mu} \sum_{n=1}^{\infty} c_n J_0(\frac{\lambda_n r}{R}) \exp(-\frac{\lambda_n^2}{R^2} \nu t), \tag{3.113}$$

and the coefficients c_n are determined by (3.103):

$$R^2 - r^2 = \sum_{n=1}^{\infty} c_n J_0(\frac{\lambda_n r}{R}) . \tag{3.114}$$

To solve Eq. (3.114), let us recall the orthogonality properties of Bessel functions as expressed by Lommel integrals

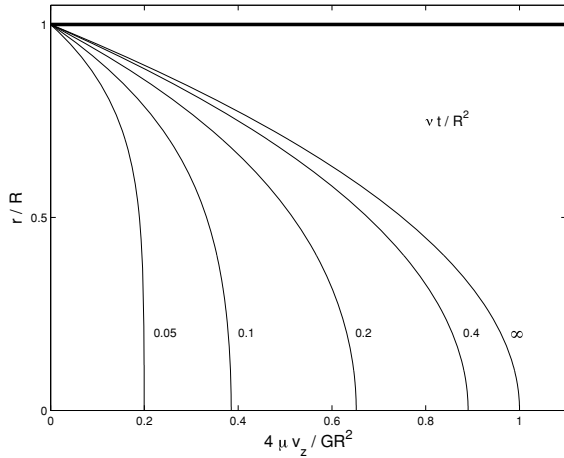$$\int_0^1 z J_n(\lambda_i z) J_n(\lambda_j z) dz = 0, \quad \lambda_i \neq \lambda_j , \tag{3.115}$$

$$\int_0^1 z J_n^2(\lambda_i z) dz = \frac{1}{2} [J_n'(\lambda_i)]^2 . \tag{3.116}$$

Solution of (3.114) is obtained with $z = r/R$ as

$$c_n = \frac{2R^2}{[J_0'(\lambda_n)]^2} \int_0^1 (1 - z^2) z J_0(\lambda_n z) dz . \tag{3.117}$$

The evaluation of the two integrals in (3.117) is carried out using successively the recurrence relationships (C.4) and then (C.3) with $\ell = 2, m = 0$. This yields

Fig. 3.10 Transient
Poiseuille flow in a circular
pipe

$$\int_0^1 z\, J_0(\lambda_n z)\, dz = \frac{1}{\lambda_n} J_1(\lambda_n) \,, \tag{3.118}$$

$$\int_0^1 z^3\, J_0(\lambda_n z)\, dz = \frac{1}{\lambda_n^4} \left[\lambda_n^3 J_1(\lambda_n) + 2\lambda_n^2 J_0(\lambda_n) - 4\lambda_n J_1(\lambda_n) \right] \,, \tag{3.119}$$

$$= \frac{1}{\lambda_n} J_1(\lambda_n) - \frac{4}{\lambda_n^3} J_1(\lambda_n) \,.$$

One finds with the help of the relation $[J_0'(\lambda_n)]^2 = [J_1(\lambda_n)]^2$: (cf. (C.5) for $m = 0$)

$$c_n = \frac{8R^2}{\lambda_n^3 J_1(\lambda_n)} \,. \tag{3.120}$$

Taking Eqs. (3.101), (3.113) and (3.120) into account, the velocity profile is

$$v_z(r,t) = \frac{G}{4\mu}\left(R^2 - r^2\right) - \frac{2GR^2}{\mu} \sum_{n=1}^{\infty} \frac{J_0(\frac{\lambda_n r}{R})}{\lambda_n^3 J_1(\lambda_n)} \exp(-\frac{\lambda_n^2}{R^2}\nu t) \,. \tag{3.121}$$

Figure 3.10 shows the velocity variation with respect to time.

3.4.2 Pulsating Flow in a Circular Pipe

Let us consider the Poiseuille flow in a circular pipe subject to the action of an
oscillating pressure gradient. This problem has been analyzed by Uchida [112] and
Womersley [122] and constitutes a modeling of the blood flow in a rigid artery, an
assumption far from physiological phenomena as arterial walls deform and move

under pressure waves [6, 127]. As the cardiac cycle is time-periodic, the pressure gradient can be represented by a Fourier series (a dozen of modes are sufficient)

$$\frac{\partial p}{\partial z} = \sum_{k=0}^{\infty} c_k e^{ik\omega t} \ . \tag{3.122}$$

The continuous component c_0 corresponds to the time average of the pressure gradient and produces the Poiseuille profile (3.47). In (3.122), ω is the signal frequency such that $\omega = 2\pi/T$, with T the period of the phenomenon. The pressure gradient corresponds to the real part of the complex representation. The flow governing equation is obtained from (A.23)

$$-\frac{\partial p}{\partial z} + \mu \left(\frac{\partial^2 v_z}{\partial r^2} + \frac{1}{r} \frac{\partial v_z}{\partial r} \right) = \rho \frac{\partial v_z}{\partial t} \ , \tag{3.123}$$

and the solution is sought in terms of the Fourier series

$$v_z(r,t) = \sum_{k=0}^{\infty} \hat{w}_k(r) \, e^{ik\omega t} \ . \tag{3.124}$$

Inserting (3.124) in (3.123), one gets

$$\frac{d^2 \hat{w}_k}{dr^2} + \frac{1}{r} \frac{d \hat{w}_k}{dr} - \frac{i\omega k}{\nu} \hat{w}_k = \frac{c_k}{\mu} \ . \tag{3.125}$$

The boundary conditions are

$$\frac{d \hat{w}_k}{dr} \mid_{r=0} = 0, \quad \hat{w}_k \mid_{r=R} = 0 \ . \tag{3.126}$$

The particular solution of (3.125) is quickly found as $-\frac{i\omega k}{\nu} \hat{w}_k = \frac{c_k}{\mu}$.

Introducing the dimensionless variable $z = r/R$, the homogeneous equation becomes

$$\frac{d^2 \hat{w}_k}{dz^2} + \frac{1}{z} \frac{d \hat{w}_k}{dz} - \frac{i R^2 \omega k}{\nu} \hat{w}_k = 0 \ , \tag{3.127}$$

whose solution is given by

$$\hat{w}_{kh} = C_1 J_0(\alpha \sqrt{k} z \, i^{3/2}) + C_2 Y_0(\alpha \sqrt{k} z \, i^{3/2}) \ , \tag{3.128}$$

where the quantity α is the dimensionless Womersley number

$$\alpha = R \sqrt{\frac{\omega}{\nu}} \ . \tag{3.129}$$

The Womersley number is the ratio of the radius to the penetration depth and is a characteristic feature of pulsatile blood flow. Typical values of α in the aorta range from 20 for a human in good health to 8 for a cat. Another way of interpreting the Womersley number consists in estimating the distance from the rigid wall, say δ, where the viscous forces and the inertia are of equal magnitude. Near the wall, viscosity is dominant and a rough estimate of the viscous forces is $\mu U/\delta^2$. Near the symmetry axis, inertia dominates and yields the estimate $\rho \omega U$. Equating the two forces leads to the definition

$$\delta^2 = \frac{\nu}{\omega} \,. \tag{3.130}$$

Therefore

$$\alpha = \frac{R}{\delta} \,. \tag{3.131}$$

If α is large, the viscous effects are confined to a region very close to the wall. In the centre of the flow, the dynamics will be driven by the equilibrium of inertia and pressure forces, resulting in a velocity profile that will be more blunt than the parabolic profile that comes from the balance of viscous and pressure forces.

The functions J_0 and K_0 with the complex argument are Kelvin functions of order zero [1]. As the boundary conditions impose a finite velocity on the axis, it follows that $C_2 \equiv 0$ because Y_0 and $Y_0' \to \infty$ when $r \to 0$. The velocity profile is

$$v_z(r, t) = -\frac{c_0}{4\mu} R^2 \left(1 - (\frac{r}{R})^2 \right)$$
$$+ \frac{R^2}{\mu} \sum_{k=1}^{\infty} \Re \left(\frac{ic_k}{\alpha_k^2} \left[1 - \frac{J_0(\alpha_k \frac{r}{R} i^{3/2})}{J_0(\alpha_k i^{3/2})} \right] e^{ik\omega t} \right) \,. \tag{3.132}$$

In this last relation, we have set $\alpha_k = \alpha \sqrt{k}$. The complex function $J_0(z\, i^{3/2})$ with z real ≥ 0 is decomposed in a real part $Ber(z)$ (real Bessel) and an imaginary part $Bei(z)$ (imaginary Bessel) such that

$$J_0(z\, i^{3/2}) = Ber(z) + i\, Bei(z) \,, \tag{3.133}$$

and the final velocity profile reads

$$v_z(r, t) = -\frac{c_0}{4\mu} R^2 \left(1 - (\frac{r}{R})^2 \right)$$
$$+ \frac{R^2}{\mu} \sum_{k=1}^{\infty} \Re \left(\frac{ic_k}{\alpha_k^2} \left[1 - \frac{Ber(\alpha_k \frac{r}{R}) + i\, Bei(\alpha_k \frac{r}{R})}{Ber(\alpha_k) + i\, Bei(\alpha_k)} \right] e^{ik\omega t} \right) \,. \tag{3.134}$$

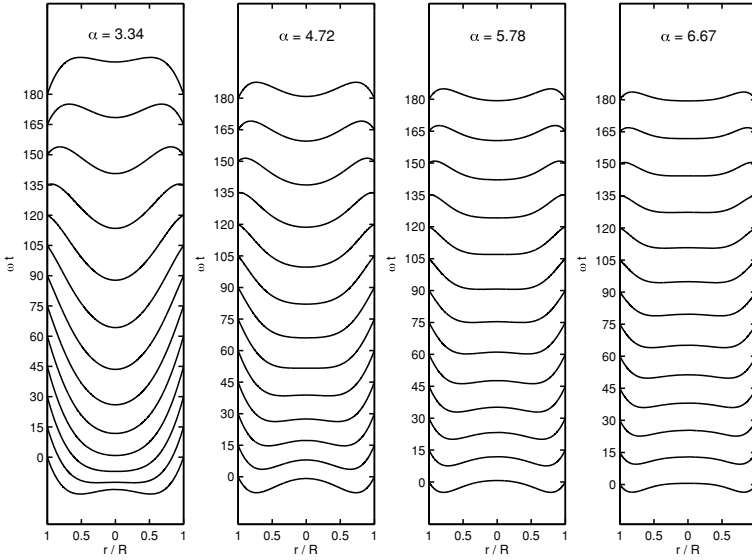The velocity profile for mode $k = 1$ is shown in Fig. 3.11 for Womersley numbers between 3.34 and 6.67.

Fig. 3.11 Pulsatile velocity profile for various values of the Womersley number

The flow rate across the pipe section is given by

$$Q = 2\pi \int_0^R v_z(r, t)\, r\, dr$$

$$= -\frac{c_0}{8\mu}\pi R^4 + \frac{\pi R^4}{\mu} \sum_{n=1}^{\infty} \Re\left(\frac{ic_k}{\alpha_k^2} F(\alpha_k) e^{ik\omega t}\right) , \qquad (3.135)$$

$$F(\alpha_k) = 1 - 2J_1(\alpha_k\, i^{3/2})/\left[\alpha_k\, i^{3/2} J_0(\alpha_k\, i^{3/2})\right] . \qquad (3.136)$$

The cases of slow and rapid pulsation are interesting limit cases.

3.4.2.1 Slow Pulsation

In this case, α is supposed to be small. The Taylor series of (3.133) (cf. [1]) is

$$J_0(z\, i^{3/2}) = 1 - \frac{(z/2)^4}{(2!)^2} + \frac{(z/2)^8}{(4!)^2} - \frac{(z/2)^{12}}{(6!)^2} \cdots$$

$$+ i\left(\frac{(z/2)^2}{(1!)^2} - \frac{(z/2)^6}{(3!)^2} - \frac{(z/2)^{10}}{(5!)^2} - \cdots\right) . \qquad (3.137)$$

Taking the dominant terms into account, one obtains successively

$$\frac{J_0(\alpha_k \frac{r}{R} i^{3/2})}{J_0(\alpha_k i^{3/2})} = \frac{1 + i\frac{(\alpha_k \frac{r}{R})^2}{4} - \frac{(\alpha_k \frac{r}{R})^4}{64} + \cdots}{1 + i\frac{\alpha_k^2}{4} - \frac{\alpha_k^4}{64}} . \tag{3.138}$$

Developing the inverse of the denominator, one has

$$(1 + i\frac{\alpha_k^2}{4} - \frac{\alpha_k^4}{64})^{-1} = 1 - i\frac{\alpha_k^2}{4} - \frac{\alpha_k^4}{16} + \frac{\alpha_k^4}{64} + \cdots$$

$$\simeq 1 - \frac{i\alpha_k^2}{4} - \frac{3\alpha_k^4}{64} . \tag{3.139}$$

Eventually we write

$$\frac{J_0(\alpha_k \frac{r}{R} i^{3/2})}{J_0(\alpha_k i^{3/2})} = 1 - i\frac{\alpha_k^2}{4}\left(1 - (\frac{r}{R})^2\right) - \frac{\alpha_k^4}{64}\left((\frac{r}{R})^4 - 4(\frac{r}{R})^2 + 3\right) + O(\alpha_k^6) . \tag{3.140}$$

The velocity is now

$$v_z(r,t) = -\frac{c_0}{4\mu}R^2\left(1 - (\frac{r}{R})^2\right) - \frac{R^2}{\mu}\sum_{k=1}^{\infty}\frac{c_k}{4}\left(1 - (\frac{r}{R})^2\right)\cos(k\omega t)$$

$$+ \frac{c_k\alpha_k^2}{64}\left((\frac{r}{R})^4 - 4(\frac{r}{R})^2 + 3\right)\sin(k\omega t) . \tag{3.141}$$

If the continuous Poiseuille component of the velocity is neglected and if we set $v_{z,c} = -c_1 R^2/(4\mu)$ and $\alpha_1 = \alpha$, the first mode $k = 1$ becomes

$$\frac{v_z}{v_{z,c}} = \left(1 - (\frac{r}{R})^2\right)\cos(\omega t) + \frac{\alpha^2}{16}\left((\frac{r}{R})^4 - 4(\frac{r}{R})^2 + 3\right)\sin(\omega t) . \tag{3.142}$$

The flow comprises a Poiseuille part in phase with the imposed pressure gradient and this is perfectly logical as the pulsation is slow and therefore, the flow has time to adjust itself to that variation. The additional term presents a phase shift of $\pi/2$. Figure 3.12 shows the velocity profile for values of $\alpha = 1/\sqrt{2}$ and $\omega t = 0, \pi/4, \pi/2, 3\pi/4$. Starting from the Poiseuille flow at time $\omega t = 0$, at mid period ($\omega = \pi/2$), the profile is still positive while the corresponding pressure gradient vanishes. The phase difference disappears at mid cycle ($\omega t = \pi$) and the Poiseuille flow is recovered.
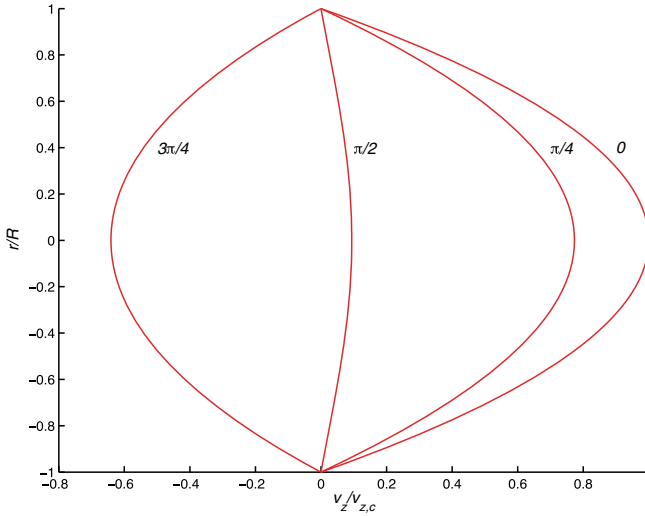
Fig. 3.12 Slow pulsatile flow with $\alpha^2 = 1/2$

3.4.2.2 Rapid Pulsation

The parameter $\alpha r/R$ takes large values and the axis ($r = 0$) is excluded from the analysis. For high values of its argument, the asymptotic development of $J_0(z)$ (cf. Eq. (14.144) of Arfken et al. [3]) is such that

$$J_0(z) = \sqrt{\frac{2}{\pi z}} \cos\left(z - \frac{\pi}{4}\right) + O(|z|^{-1}), \quad \text{with} \quad |arg(z)| < 2\pi . \qquad (3.143)$$

Using the relation $i^{3/2} = e^{i3\pi/4}$ and $s = \alpha_k r/R$, we perform the next algebraic calculation

$$J_0(e^{i3\pi/4}s) = e^{-i3\pi/8}\sqrt{\frac{2}{\pi s}} \cos\left(e^{i3\pi/4}s - \frac{\pi}{4}\right)$$

$$= e^{-i3\pi/8}\sqrt{\frac{2}{\pi s}} \left(\cos\left(i\frac{s}{\sqrt{2}}\right) - \left(\frac{s}{\sqrt{2}} + \frac{\pi}{4}\right)\right)$$

$$= e^{-i3\pi/8}\sqrt{\frac{2}{\pi s}} \left(\cos\left(i\frac{s}{\sqrt{2}}\right)\cos\left(\frac{s}{\sqrt{2}} + \frac{\pi}{4}\right) + \sin\left(i\frac{s}{\sqrt{2}}\right)\sin\left(\frac{s}{\sqrt{2}} + \frac{\pi}{4}\right)\right)$$

$$= e^{-i3\pi/8}\sqrt{\frac{2}{\pi s}} \left(\cosh\left(\frac{s}{\sqrt{2}}\right)\cos\left(\frac{s}{\sqrt{2}} + \frac{\pi}{4}\right) + i\sinh\left(\frac{s}{\sqrt{2}}\right)\sin\left(\frac{s}{\sqrt{2}} + \frac{\pi}{4}\right)\right)$$

$$= e^{-i3\pi/8}\sqrt{\frac{2}{\pi s}} \cosh\left(\frac{s}{\sqrt{2}} + i\left(\frac{s}{\sqrt{2}} + \frac{\pi}{4}\right)\right) .$$

Neglecting the decaying exponential in cosh as we deal with large values of the argument, we obtain

$$J_0(e^{i3\pi/4}s) = e^{-i3\pi/8}\sqrt{\frac{1}{2\pi s}}e^{\frac{s}{\sqrt{2}}}e^{i\left(\frac{s}{\sqrt{2}}+\frac{\pi}{4}\right)} . \tag{3.144}$$

Consequently one finds

$$\frac{J_0(\alpha_k \frac{r}{R} i^{3/2})}{J_0(\alpha_k i^{3/2})} \approx \frac{1}{\sqrt{r/R}}e^{-(1+i)\frac{\alpha_k}{\sqrt{2}}(1-\frac{r}{R})} . \tag{3.145}$$

The first mode of the velocity profile in absence of the continuous Poiseuille component yields

$$\frac{v_z}{v_{z,c}} = \frac{4}{\alpha^2}\left[\sin(\omega t) - \frac{1}{\sqrt{r/R}}e^{-\frac{\alpha}{\sqrt{2}}(1-\frac{r}{R})}\sin\left(\omega t - \frac{\alpha}{\sqrt{2}}(1-\frac{r}{R})\right)\right] + O\left(\frac{1}{\alpha^4}\right) . \tag{3.146}$$

We observe that the resulting flow is in complete phase shift by a factor of $\pi/2$ with respect to the pressure gradient. We must again draw the attention of the reader to the assumptions of this approximation which bans the presence of the axis.

3.5 Plane Periodic Solutions

Many exact solutions of the Navier–Stokes equations are obtained for spatial periodic conditions. In this section we consider a two-dimensional (2D) solution due to Walsh [117].

Let us first proof the following theorem.

Theorem 3.1 (Walsh) *Let us consider a vector field $\boldsymbol{u}$ in the domain Ω that satisfies*

$$\nabla^2 \boldsymbol{u} = \lambda\,\boldsymbol{u}, \tag{3.147}$$

$$\text{div } \boldsymbol{u} = 0 . \tag{3.148}$$

Then the velocity $\boldsymbol{v} = e^{\nu\lambda t}\boldsymbol{u}$ satisfies the Navier–Stokes equations (1.73)–(1.74) with a pressure p such that

$$\nabla p = -\boldsymbol{v} \cdot \nabla \boldsymbol{v} . \tag{3.149}$$

The vector $\boldsymbol{v}$ is divergence free as is also $\boldsymbol{u}$. Furthermore,

$$\frac{\partial \boldsymbol{v}}{\partial t} = \nu\lambda\boldsymbol{v} = \nu\Delta\boldsymbol{v} . \tag{3.150}$$

It remains to prove that the nonlinear term is a gradient, i.e. that $\nabla \times (\boldsymbol{v} \cdot \nabla \boldsymbol{v}) = 0$. This amounts to showing that

$$\frac{\partial}{\partial x_2}\left(v_1 \frac{\partial v_1}{\partial x_1} + v_2 \frac{\partial v_1}{\partial x_2}\right) = \frac{\partial}{\partial x_1}\left(v_1 \frac{\partial v_2}{\partial x_1} + v_2 \frac{\partial v_2}{\partial x_2}\right), \qquad (3.151)$$

as **curl ∇ = 0**. This is evident by incompressibility and relation (3.150).

In the 2D case, we resort to the streamfunction ψ, assuming that it is an eigenfunction of the Laplacian with eigenvalue λ. Consequently, $\boldsymbol{u} = (\partial\psi/\partial x_2, -\partial\psi/\partial x_1)$ satisfies (3.147)–(3.148) with the same λ. Therefore, $e^{\nu\lambda t}\psi$ is the streamfunction of the associated Navier–Stokes flow. If we have a periodic domain of size 2π, then the eigenvalues λ are of the form $\lambda = -(k_{x_1}^2 + k_{x_2}^2)$, with k_{x_1} and k_{x_2} positive integers. For given k_{x_1}, k_{x_2}, the linearly independent eigenfunctions are

$$\cos(k_{x_1}x_1)\cos(k_{x_2}x_2), \ \sin(k_{x_1}x_1)\sin(k_{x_2}x_2),$$
$$\cos(k_{x_1}x_1)\sin(k_{x_2}x_2), \ \sin(k_{x_1}x_1)\cos(k_{x_2}x_2).$$

It is possible to build up complicated geometrical patterns by combination of the eigenfunctions named n, m eigenfunction by Walsh, with $\lambda = -(n^2 + m^2)$. A theorem in number theory shows that integers of the form p^{2i} and p^{2i+1}, where p is an integer prime number such that $p \equiv 1 \pmod 4$, may be written as sums of squares in exactly $i + 1$ manners. For example, $625 = 5^4 = 25^2 = 24^2 + 7^2 = 20^2 + 15^2$. Figure 3.13 displays the streamlines corresponding to $\psi = \sin(25x_1) + \cos(25x_2) - \sin(24x_1)\cos(7x_2) + \cos(15x_1)\cos(20x_2) - \cos(7x_1)\sin(24x_2)$.
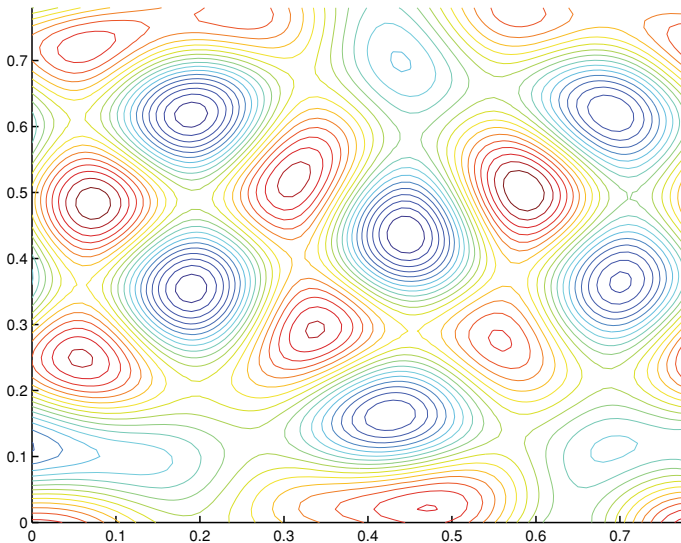

Fig. 3.13 ψ isocontours in the square $(0, \pi/4)^2$

3.6 Pipe Flow

Engineering and industrial applications require very often to move various fluids flowing through pipes: oil, water, grain, etc. To model that situation, we will consider a steady state laminar longitudinal flow in a pipe of arbitrary section in order to obtain afterwards the optimal shape of the pipe. The material presented in this section is much influenced by the book by Langlois and Deville [49].

Let x_3 be the axis of the Cartesian coordinate system parallel to the pipe generatrix. Let us assume that a mechanical device like a pump generates a constant pressure gradient G such that $-\partial p / \partial x_3 = G$. This pressure gradient gives rise to a rectilinear laminar flow along the pipe. Therefore, the velocity profile is

$$v_1 = v_2 = 0, \quad v_3 = v_3(x_1, x_2) . \tag{3.152}$$

It is easily verified that the continuity Eq. (1.73) is satisfied and also the Navier–Stokes equations (1.74) in directions x_1 and x_2. If the body force is constant, the third Navier–Stokes equation yields

$$\Delta v_3 + \frac{G}{\mu} = 0 , \tag{3.153}$$

where $G = G' + \rho b_3$ with the assumption that $p = C - G' x_3$, $C = cnst$ and Δ is the two-dimensional Laplacian, i.e.

$$\Delta = \frac{\partial^2}{\partial x_1^2} + \frac{\partial^2}{\partial x_2^2} . \tag{3.154}$$

Equation (3.153) is a special case of Poisson's equation, a linear, second-order partial differential equation of the elliptic type. We shall look for solutions which satisfy the boundary condition

$$v_3(x_1, x_2) = 0 \quad \text{on } \Gamma , \tag{3.155}$$

where Γ is the periphery of the pipe cross section.

The boundary value problem represented by (3.153) and (3.155) is equivalent to the Dirichlet problem

$$\nabla^2 u = 0 , \tag{3.156}$$
$$u = f(x_1, x_2) \quad \text{on } \Gamma . \tag{3.157}$$

To show the equivalence, we need only set

$$v_3(x_1, x_2) = \frac{G}{2\mu} [u(x_1, x_2) - f(x_1, x_2)] , \tag{3.158}$$

where f is *any* function satisfying

$$\Delta f = 2 \, . \tag{3.159}$$

3.6.1 Polynomial solutions

Many polynomials have constant Laplacian; some of these, when equated to zero,
yield the equation of a closed contour. Thus setting $v_3(x_1, x_2)$ equal to such a poly-
nomial, multiplied by an appropriate constant, will satisfy (3.153) and (3.155), with
Γ the contour on which the polynomial vanishes. We reject immediately all linear
polynomials for two reasons: they vanish only on straight lines, not on closed con-
tours; their Laplacians are not only constant, they vanish. Consideration of quadratic
polynomials, however, bears fruit.

3.6.1.1 The Elliptical Pipe

We note first that the Laplacian of any quadratic polynomial is constant. We next
recall that equating any quadratic polynomial to zero yields the equation of a conic
section. Only the ellipses are of interest to us, for circles were treated in the Sect. 3.2.2
and none of the other conic sections are closed contours. The algebra is simplified by
placing the centroid of the ellipse on the x_3-axis, and orienting the x_1- and x_2-axes
along the axes of the ellipse as shown in Fig. 3.14. Thus the most general ellipse can
be represented by

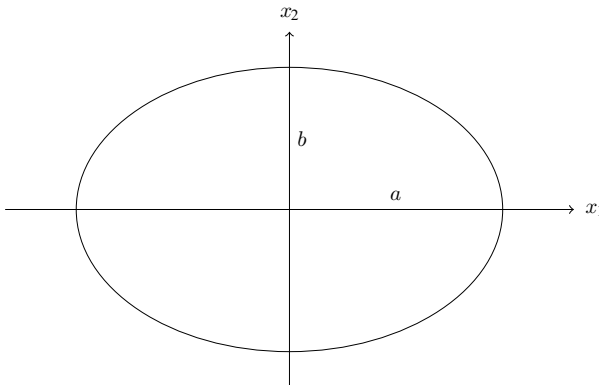$$\left(\frac{x_1}{a}\right)^2 + \left(\frac{x_2}{b}\right)^2 = 1 \, . \tag{3.160}$$

Fig. 3.14 Elliptic pipe

We find by inspection that a solution to (3.153) which vanishes on the ellipse (3.160) is provided by

$$v_3 = \frac{G}{2\mu} \frac{a^2 b^2}{a^2 + b^2} \left(1 - \frac{x_1^2}{a^2} - \frac{x_2^2}{b^2} \right) .$$

(3.161)

The volume flow rate is easily calculated. We have

$$Q = \int \int v_3 \, dx_1 dx_2 ,$$

(3.162)

where the integration is carried out over the ellipse. With (3.161),

$$Q = \frac{\pi G}{4\mu} \frac{a^3 b^3}{a^2 + b^2} .$$

(3.163)

This result may be rewritten

$$Q = \frac{G A^2}{4\pi \mu} \frac{R}{1 + R^2} ,$$

(3.164)

where $A = \pi ab$ is the area of the ellipse and $R = a/b$ is the ratio of the semi-axes. We then obtain

$$\frac{\partial Q}{\partial R} = \frac{G A^2}{4\pi \mu} \frac{1 - R^2}{(1 + R^2)^2} .$$

(3.165)

Hence, for μ, G, A all fixed, Q has an extremum at $R = 1$, which is easily shown to be a maximum. We thus find that the circular pipe is more efficient than any elliptical pipe, in the sense that the circular pipe produces a greater volume flow for a given pressure gradient than does an elliptical pipe of the same cross-sectional area.

3.6.1.2 The Triangular Pipe

It seems surprising that we can express in closed form the flow through so unlikely a cross section as an equilateral triangle, but such is the way of polynomial methods. If we place the origin at the intersection of the medians and let the negative x_1-axis pass through one vertex as in Fig. 3.15, the equation of an equilateral triangle with height $3a$ becomes

$$(x_1 - a)(x_1 - \sqrt{3}\, x_2 + 2a)(x_1 + \sqrt{3}\, x_2 + 2a) = 0 .$$

(3.166)

Note that the two last parentheses in (3.166) are the equations for the two slanted sides of the triangle. Since

Fig. 3.15 Triangular pipe
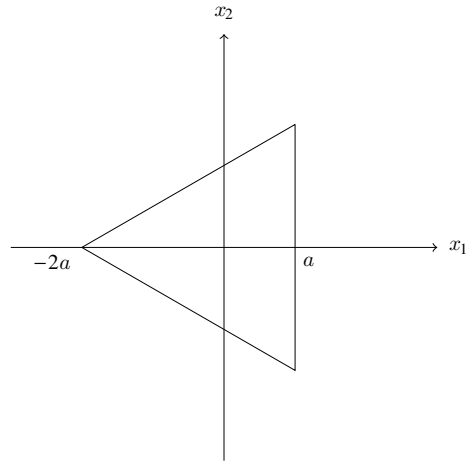
$$\Delta \left[(x_1 - a)(x_1 - \sqrt{3}\, x_2 + 2a)(x_1 + \sqrt{3}\, x_2 + 2a) \right] = 12a \, , \qquad (3.167)$$

we have

$$v_3 = \left(\frac{G}{12a\mu} \right) (a - x_1)(x_1 - \sqrt{3}\, x_2 + 2a)(x_1 + \sqrt{3}\, x_2 + 2a) \, . \qquad (3.168)$$

It is readily verified that the maximum velocity occurs at the origin, and that its value there is $Ga^2/3\mu$.

3.6.2 The Rectangular Pipe

The flow in a rectangular pipe cannot be solved using the previous approach of polynomial solutions as the equation of a rectangle does not have constant Laplacian. Here we resort to the method of separation of variables.

The rectangular section of the pipe has sides $2a$ and $2b$ and is depicted in Fig. 3.16.

The governing equation (3.153) is subjected to the boundary condition

$$v_3 = 0 \quad \text{on} \quad x_1 = \pm a \quad \text{and} \quad x_2 = \pm b \, . \qquad (3.169)$$

The solution of (3.153) is decomposed in a particular solution v_{3p} taking the constant term into account and a homogeneous periodic solution v_{3h} of the equation

$$\Delta v_{3h} = 0 \, . \qquad (3.170)$$

Fig. 3.16 Rectangular pipe
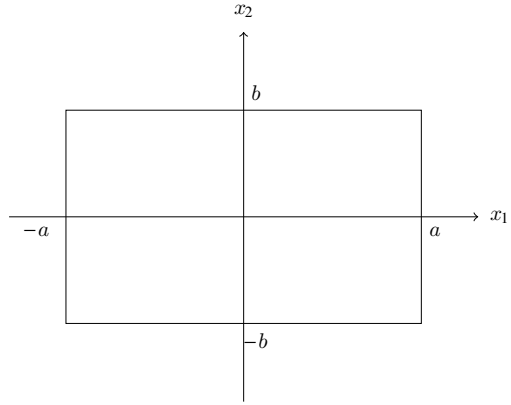
The particular solution is provided by the plane Poiseuille problem (3.27) written as

$$v_{3p} = \frac{G}{2\mu} \left(b^2 - x_2^2 \right) \ . \tag{3.171}$$

Consequently the homogeneous solution must satisfy the boundary conditions

$$v_{3h} = \frac{G}{2\mu} (x_2^2 - b^2) \quad \text{on } x_1 = \pm a \ , \tag{3.172}$$

$$v_{3h} = 0 \quad \text{on } x_2 = \pm b \ . \tag{3.173}$$

The homogeneous solution of (3.170) is obtained by separation of variables such that

$$v_{3h} = \sum_{n=0}^{\infty} X_n(x_1) Y_n(x_2) \ . \tag{3.174}$$

One has

$$\frac{X_n''}{X_n} = -\frac{Y_n''}{Y_n} = k_n^2 \ . \tag{3.175}$$

The Y_n solution reads

$$Y_n(x_2) = \cos k_n x_2 \ . \tag{3.176}$$

With the boundary condition (3.173), the coefficient k_n is obtained as $k_n = (2n + 1)\pi/(2b)$. The corresponding $X_n(x_1)$ is determined from

$$\frac{X_n''}{X_n} = k_n^2 \ , \tag{3.177}$$

i.e.,

$$X_n = A_n \cosh k_n x_1 + B_n \sinh k_n x_1 .$$
$$(3.178)$$

Because of the symmetry of the problem, we have $B_n = 0$. Thus we let

$$v_{3h}(x_1, x_2) = \sum_{n=0}^{\infty} A_n \cosh k_n x_1 \cos k_n x_2 ,$$
$$(3.179)$$

and set about determining the coefficients A_n so as to satisfy the boundary conditions (3.172). With the symmetry of the hyperbolic cosine, we need

$$\sum_{n=0}^{\infty} A_n \cosh[(n + \frac{1}{2}) \frac{\pi a}{b}] \cos k_n x_2 = \frac{G}{2\mu}(x_2^2 - b^2) .$$
$$(3.180)$$

The cosine functions are orthogonal in Fourier analysis. They satisfy the relation

$$\frac{1}{b} \int_{-b}^{b} \cos k_n x_2 \, \cos k_m x_2 \, dx_2 = \delta_{mn} .$$
$$(3.181)$$

Multiplying the two sides of (3.180) by $\cos k_m x_2$ and integrating, we have

$$A_m \cosh[(m + \frac{1}{2}) \frac{\pi a}{b}] = \frac{G}{2\mu b} \int_{-b}^{b} (x_2^2 - b^2) \, \cos k_m x_2 \, dx_2 .$$
$$(3.182)$$

Utilizing the relation

$$\int x_2^2 \cos x_2 \, dx_2 = 2x_2 \cos x_2 + (x_2^2 - 2) \sin x_2 ,$$
$$(3.183)$$

one gets

$$A_m \cosh[(m + \frac{1}{2}) \frac{\pi a}{b}] = \frac{G}{2\mu} \frac{4(-1)^{m+1}}{bk_m^3} = \frac{G}{2\mu} \frac{32(-1)^{m+1}b^2}{(2m + 1)^3\pi^3} .$$
$$(3.184)$$

The final solution reads

$$v_3 = \frac{G}{2\mu} \left[b^2 - x_2^2 + \frac{32b^2}{\pi^3} \sum_{n=0}^{\infty} \frac{(-1)^{n+1} \cosh(2n + 1)\frac{\pi x_1}{2b} \cos(2n + 1)\frac{\pi x_2}{2b}}{(2n + 1)^3 \cosh(2n + 1)\frac{\pi a}{2b}} \right] .$$
$$(3.185)$$

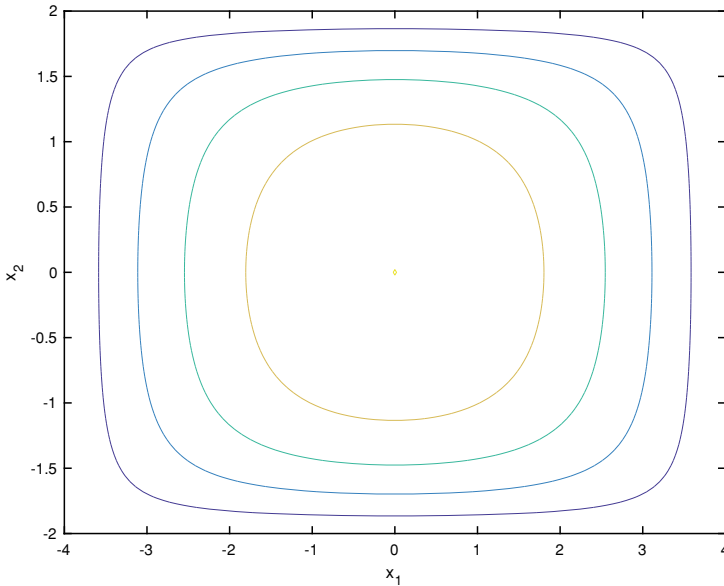Figure 3.17 shows isocontour lines for $v_3/v_{max} = cst$ in a channel of rectangular section with $a = 2b = 4$.

Fig. 3.17 $v_3/v_{max} = 0.2, 0.4, 0.6, 0.8, 1.0$ isocontours for a rectangular section with $a = 2b = 4$

Exercises

3.1 Consider the two-dimensional Couette–Poiseuille flow obtained by superimposing Couette flow induced by the constant velocity motion U of the upper wall and Poiseuille flow resulting from a pressure gradient in direction x_1. Calculate the velocity profile, the shear stress, and the flow rate.

3.2 A solid sphere of radius R is immersed in an incompressible viscous Newtonian fluid that fills the space and is at rest at infinity. The sphere rotates about its diameter at a constant angular velocity Ω. Assume that the Reynolds number is less than one and neglect the volume forces. The streamlines are circles centered on the rotation axis in planes perpendicular to this axis. Working in spherical coordinates, calculate the velocity profile.

3.3 With the same hypotheses as in the preceding exercise, examine the flow of a fluid between two spheres of radii R_1 and R_2 such that $R_1 < R_2$, which rotate at the angular velocities Ω_1 and Ω_2 about a common, fixed axis. Calculate the velocity profile. This solution is called the spherical Couette flow.

3.4 A cylinder of radius R_1 moves parallel to its axis with a constant velocity U inside a fixed, coaxial cylinder of radius R_2.

Calculate the velocity field of a viscous fluid which fills the space between the two cylinders. Find the friction force per unit length that acts on the moving cylinder.
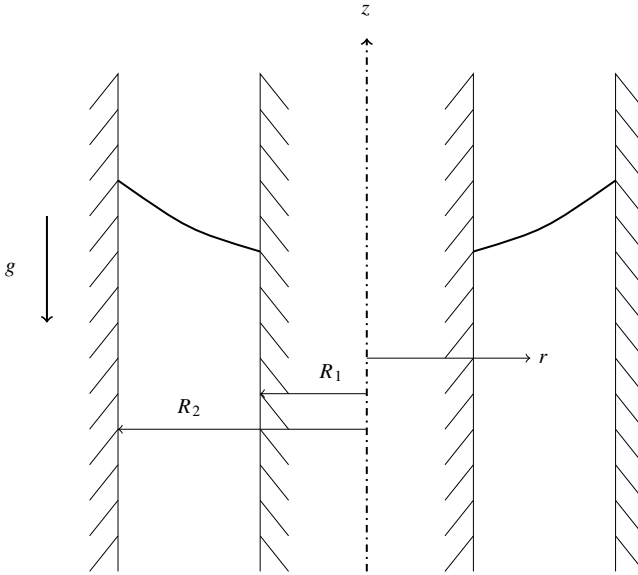
Fig. 3.18   Couette flow with free surface

3.5 Couette flow with a free surface

Consider the circular Couette flow between two cylinders. The viscous fluid fills the annular space under a free surface that is in contact with the ambient air assumed to behave as an inviscid fluid. Figure 3.18 shows the Couette device.

The outer cylinder rotates with the velocity $v_\theta(R_2) = \omega_2 R_2$, while the inner cylinder rotates at velocity $v_\theta(R_1) = \omega_2 R_1$.

- Compute the fluid velocity.
- Compute the shape of the free surface $z = z(r)$. The free surface is an isobar where the pressure is equal to the atmospheric pressure p_a. The fluid height on the inner cylinder is given by $z(R_1) = z_1$.

3.6 Plane Couette flow with two layers

We consider the plane Couette flow of two incompressible fluids of different viscosities and densities as shown in Fig. 3.19. The steady flow is oriented in direction x_1 and is generated by the upper wall moving with constant velocity U. The two layers of height h_1 and h_2, respectively, do not mix and the interface is positioned at $x_2 = 0$. The bottom wall is fixed. It is assumed that no pressure gradient influences the flow.

Evaluate the velocity field and the resulting vorticity.

3.7 Bubble dynamics

A spherical bubble of inviscid gas is contained in an infinite volume of viscous fluid. We suppose that the pressure p_g of the gas inside the bubble varies with time. As a consequence the radius R of the bubble will also vary with time. The varying

Fig. 3.19 Plane Couette flow with two immiscible fluids
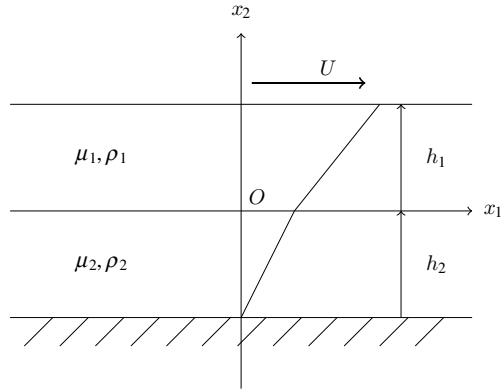
bubble generates a velocity field within the fluid which in turn generates a stress field.

Compute the velocity v_r, the pressure distribution in the fluid, the governing equation for the bubble dynamics and investigate the treatment of the interface.